10 July 2002

Chemical Physics Letters 360 (2002) 195–201

CHEMICAL PHYSICS LETTERS

www.elsevier.com/locate/cplett

Triplet formation and decay in conjugated polymer devices

A.S. Dhoot [a], D.S. Ginger [a], D. Beljonne [b], Z. Shuai [b,1], N.C. Greenham [a,*]

[a] *Cavendish Laboratory, University of Cambridge, Madingley Road, Cambridge CB3 0HE, UK*

[b] *Service de Chimie des Matériaux Nouveaux, Université de Mons-Hainaut, 20 Place du Parc, B-7000 Mons, Belgium*

Received 18 January 2002

Abstract

We have studied infrared absorptions in working polymer light-emitting diodes due to the presence of polarons and triplet excitons. The polaron population is found to be proportional to the applied voltage, providing direct evidence for space-charge-limited currents. Measurement of triplet absorptions allows us to study the generation and decay rates for triplet excitons. At low temperatures, we find that $83 \pm 7\%$ of excitons are formed as singlets rather than triplets, and we show that interaction with polarons is an important decay mechanism for triplet excitons, with a rate constant of 3×10^{-14} cm^3 s^{-1}.

The decay of excitons formed by charge-carrier recombination in conjugated polymers is of fundamental importance in the operation of polymer-based electronic devices such as polymer light-emitting diodes (LEDs). Improved understanding of electronic processes in conjugated polymers has allowed LED performance to be improved to levels where commercial applications are attractive [1], however many details of the exciton formation and decay processes remain unclear. When positive and negative charge-carriers recombine in a polymer LED, either singlet or triplet excitons may be formed. Triplet excitons, which do not have an efficient radiative decay pathway, have been identified in polymer LEDs by magnetic resonance [2] and optical [3] measurements and by the incorporation of phosphorescent dopants [4], however it has been difficult to obtain quantitative information about triplet generation and decay rates. Simple spin statistics arguments predict that 75% of excitons are formed as triplets, thus limiting the quantum efficiency of the LED to a maximum of 25%. Recent measurements of high efficiencies in polymer LEDs suggest that fewer than 75% of excitons are formed as triplets [5–7], which makes accurate determination of triplet populations in working LEDs particularly important. Charged excitations also play an important role in polymer LEDs, since they are present in high concentrations due to their low mobility. Injected charges redistribute the electric field within the device, leading to space-charge-limited currents, and may also act as quenching sites for

* Corresponding author. Fax: +44-1223-353397.
E-mail address: ncg11@cam.ac.uk (N.C. Greenham).
[1] Current address: Institute of Chemistry, Chinese Academy of Sciences, Zhongguancun North First Street, 2100080 Beijing, PR China.

0009-2614/02/$ - see front matter
PII: S0009-2614(02)00840-0

singlet and triplet excitons. It is therefore important to measure charge populations directly in LEDs, and to study the interactions between charges and excitons.

In this Letter we perform optical spectroscopy on working polymer LEDs to study triplet excitons and charges within the devices. Due to strong structural and electronic relaxation in the excited state, charges in conjugated polymers form polaronic states which may be identified by two absorptions below the energy gap. Triplet excitons, although not coupled radiatively to the ground state, have an allowed transition to a higher-lying triplet state which leads to an absorption in the near-infrared. Previous experiments have shown that it is possible to identify either charge carriers or triplet excitons in organic LEDs using spectroscopic techniques [8–12]; our aim is to separate features due to triplet excitons, charges and extrinsic effects, and hence to obtain quantitative information about the physics of excited state formation and decay in polymer LEDs.

LEDs were fabricated by spin coating a film of poly(2-methoxy-5-(3′, 7′-dimethyl)-octyloxy-*p*-phenylenevinylene) (OC1C10-PPV) on a glass substrate prepared with a semitransparent metallic anode. Semitransparent cathodes of area 9 mm^2 were then formed by evaporating a thin layer of calcium encapsulated with 6 nm of gold. For hole-only devices, 6 nm of gold alone was used for the cathode. Devices were handled and measured under an inert atmosphere, and electrical characteristics were similar to devices with thicker cathodes. Transmission measurements were performed between 0.4 and 3.1 eV using monochromated light from a tungsten–halogen lamp. A second monochromator was used to reduce the effect of electroluminescence (EL), and the transmitted probe beam was detected using an InSb or Si photodiode. The drive voltage was modulated between 0 and V in a square wave with 50% duty cycle at frequencies from 2 Hz to 4 kHz. A lock-in amplifier was used to detect the modulation of the probe beam at the driving frequency. At each wavelength any remaining EL signal was measured by blocking the probe beam and subtracted from the total signal. The signal was normalised by the unmodulated transmission to give the fractional change in transmission ($\Delta T/T$). In order to resolve features at low energies, gold was used as the anode instead of indium-tin oxide (ITO) since ITO showed a strong electroreflectance in the range 0.5–1.2 eV, leading to a modulation in transmission which obscured the absorption features. A small additional modulation arose from electrostriction effects, where weak interference between beams reflected within the device is modulated by a change in the polymer thickness due to the electrostatic force between the electrodes. In our experiments we minimize these effects by reducing the polymer thickness, and by using thin electrodes to reduce the reflections within the device. For quantitative analysis of features due to injected excited states any remaining electrostriction signal was eliminated by subtracting spectra obtained in forward and reverse bias.

Fig. 1 shows modulation spectra for bipolar and hole-only OC1C10-PPV devices at room temperature. Two characteristic features are seen in both spectra, one peaking at 0.47 eV, the other having a broad peak in the range 1.25–2.0 eV. The features have an identical dependence on modulation voltage and frequency. Similar features are seen in photoinduced absorption (PIA) measure-

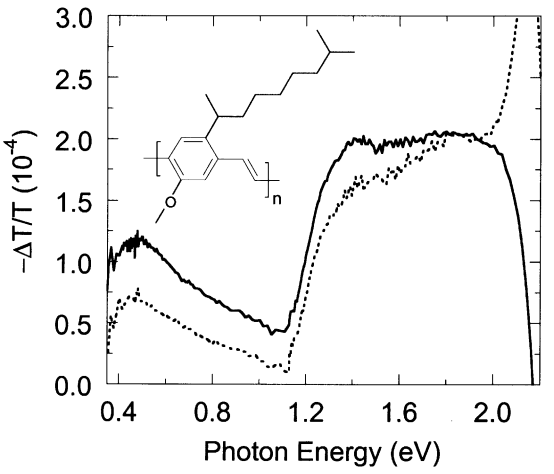

Fig. 1. Modulation spectrum of an Au/OC1C10-PPV/Ca/Au device (solid) and a Au/OC1C10-PPV/Au device (dashed) at room temperature, for $V = 3.2$ and 3 V, respectively, with $f = 113$ Hz and a polymer thickness of 100 nm for both devices. The inset shows the chemical structure of OC1C10-PPV.

ments on blends of OC1C10-PPV with electron acceptors such as C_{60} or semiconductor nanocrystals where charge separation takes place, leaving a positive charge on the polymer. (PIA data are not shown here, but are very similar to published data using poly(2-methoxy-5-(2′-ethyl)-hexyloxy-*p*-phenylenevinylene) [13,14].) We therefore assign these features to polaronic charges in the device. At room temperature we do not see any features associated with triplet excitons, due to their short lifetime at high temperatures. We note that the polarons formed after charge separation in a blend are probably associated with an opposite charge on the electron acceptor, and that this is likely to explain the differences in the details of the spectra of charges formed by charge separation in a blend and electrical injection in an LED.

Figs. 2a,b show the voltage dependence of the 1.3 eV polaron signal at room temperature for both the bipolar and hole-only devices. In both cases, the polaron signal has a linear dependence on voltage, despite the fact that the current flowing through the device changes by several orders of magnitude over this voltage range. We explain the linear voltage dependence by the presence of a space-charge-limited current in the device. For a single-carrier space-charge-limited current the injected charge, Q, required to cancel out the field at the ohmic injecting contact is given by

$$Q = \frac{3}{2}\varepsilon A\frac{V}{L}, \tag{1}$$

where ε is the dielectric constant, A is the device area and V is the voltage applied across a thickness L of polymer. We can thus extract an absorption cross-section of 7.5×10^{-17} cm^2 for the high-energy polaron feature, consistent with values reported in the few conjugated polymers where measurements in metal–insulator–semiconductor structures are possible [15]. We find that the polaron signal is independent of modulation frequency, demonstrating that all the charges are swept out of the device during the 'off' cycle. It is interesting to note that Fig. 2b shows a threshold for the onset in the polaron signal at 1.4 V, which is consistent with a simple estimate of the built-in voltage for the bipolar device. In the bipolar device, the gradient of polaron density as a function

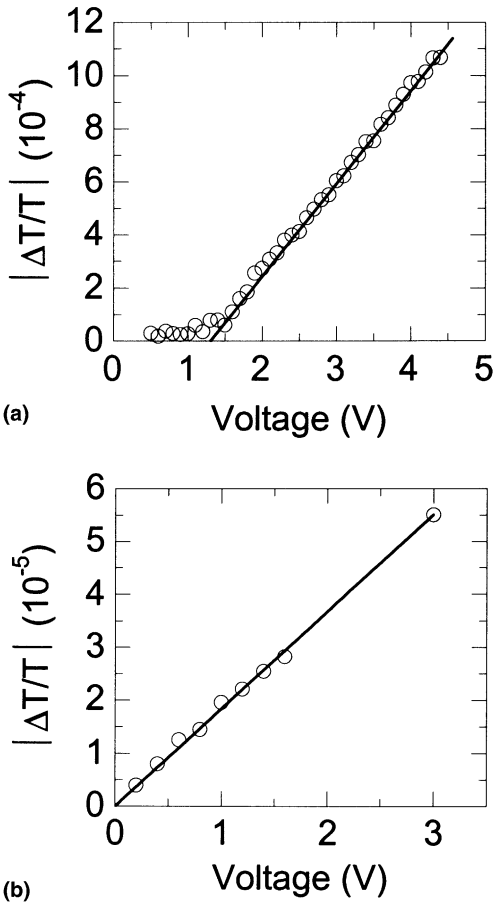

Fig. 2. The voltage dependence of the high-energy polaron signal in (a) a Au/OC1C10-PPV/Ca/Au bipolar device with polymer thickness 100 nm, and in (b) a Au/OC1C10-PPV/Au hole-only device with polymer thickness 50 nm. Both sets of data were recorded at 1.3 eV with $f = 113$ Hz at room temperature. Solid line is a linear fit to the experimental data.

of voltage is approximately twice that in the hole-only device, consistent with ohmic injection of both carriers with strong electron–hole recombination in the device.

At low temperatures we see the emergence of a sharp feature at 1.34 eV in the device spectrum as shown in Fig. 3, which is superimposed on the broad polaron signal seen at room temperature. Analysis of the in-phase and quadrature components of the lock-in signal allows the separation of these two overlapping signals due to their different decay times. The new component of the signal

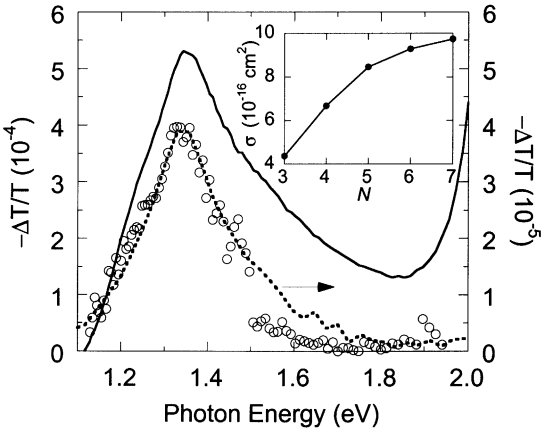

Fig. 3. Modulation spectrum of an ITO/OC1C10-PPV/Ca/Au device at 14 K (solid line) with $f = 113$ Hz, $V = 12.8$ V and a polymer thickness of 100 nm. Circles indicate the component of the signal due to triplet excitons, extracted by analysis of the phase of the total signal. The PIA spectrum (dashed line) taken for a pristine polymer film at 10 K is shown for comparison. The inset shows the calculated triplet–triplet absorption cross-section (σ) as a function of number of phenyl rings (N). The measured broadening of ~0.1 eV is used in the simulations.

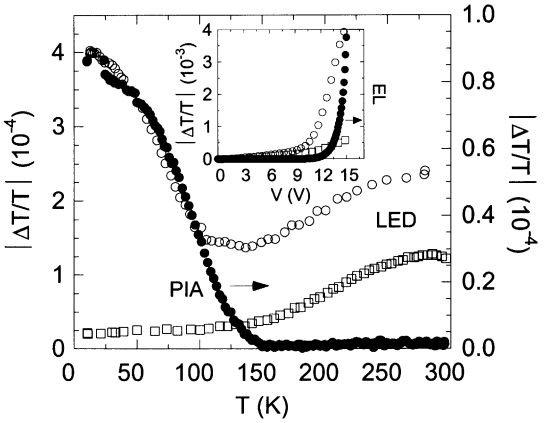

Fig. 4. Temperature dependence of the 1.35 eV (empty circles) and 0.5 eV (squares) absorptions in an LED compared with the triplet signal in PIA (filled circles). The polymer thickness was 100 nm, the modulation frequency was 113 Hz, and the devices were driven at a constant current of 500 μA. The inset shows the voltage dependence of the absorption at 1.35 eV (empty circles, predominantly triplet excitons) and 1.72 eV (squares, predominantly polarons), and the EL (filled circles) for the LED.

(Fig. 3, circles) is identical to the PIA spectrum taken for a pristine polymer film at low temperature (dashed line) where triplet excitons are generated by inter-system crossing. We therefore attribute this sharp feature to electrically generated triplet excitons. Further evidence for this assignment is given by the frequency dependence of the signal, which is consistent with monomolecular decay with a lifetime of 250 μs at low voltages, similar to the triplets seen in PIA measurements. Fig. 4 shows the temperature dependence of the triplets and polarons in the device and the triplets in the PIA. Above ~150 K, the absorption in the device at 1.35 eV follows the 0.5 eV polaron signal. As temperature drops below ~150 K, however, the 1.35 eV signal begins to rise. The increase occurs simultaneously with the sharp onset of the triplet signal in PIA, consistent with the assignment of the absorption at 1.35 eV to a combination of triplets and polarons. The triplet absorption in the device therefore behaves nearly identically to that found in PIA, and is easily distinguishable from the overlapping polaron absorption. In contrast to the polaron signal, the triplet signal increases superlinearly with voltage, approximately in proportion to the EL (inset of Fig. 4). By measurement of the magnitude and lifetime of the triplet signal as a function of voltage, we find that the triplet generation rate is indeed proportional to the EL signal, demonstrating that singlet and triplet excitons are formed in the same process in fixed proportions.

To determine triplet generation rates from our data requires knowledge of the triplet–triplet absorption cross-section. Pulse radiolysis measurements on a series of dialkoxy-phenylenevinylene polymers provide a cross-section of 1.6×10^{-15} cm^2 [16] with an uncertainty of 20%, consistent with other estimates of approximately 10^{-15} cm^2 [17,18]. To gain confidence in this rather high value, we have performed coupled-cluster quantum-chemical calculations [19,20] (including single and double excitations) to determine the oscillator strength for this transition in a series of dialkoxy-phenylenevinylene oligomers with N phenyl rings, where $N = 3$–7. The calculations yield a single, strongly allowed triplet–triplet transition, with an optical cross-section increasing from $\sim 3 \times 10^{-16}$ to $\sim 1 \times 10^{-15}$ cm^2 when going

from $N = 3$ to $N = 7$, as shown in the inset of Fig. 2 [21]. Although these calculations consistently overestimate the energy of the transition (probably because they treat isolated molecules and therefore do not include polarization effects induced by the medium), the cross-sections predicted in long oligomers (where the cross-section is beginning to saturate) are in excellent agreement with the experimental results [16,22]. Using the cross-section of Candeias et al. [16] and our measured triplet lifetime we obtain a triplet generation rate, which we then compare with the singlet generation rate determined from the measured light output using a transfer matrix model for the optical structure of the device. We allow for absorption in the electrodes and for the effect of optical interference on the radiative rate for singlet excitons. We assume that, in the absence of modification of the radiative rate, singlet states formed in the LED decay radiatively with an efficiency equal to the measured photoluminescence efficiency of OC1C10-PPV (9% at 12 K). For example, at 6.5 V and 12 K, $-\Delta T/T$ is 8.0×10^{-4} and the triplet lifetime is 142 μs, corresponding to a triplet generation rate of 3.3×10^{14} s^{-1}. From our optical model, we find that the sum of the light output in forward and reverse directions (5.4×10^{14} photons s^{-1} sr^{-1}) corresponds to a singlet exciton generation rate of 1.5×10^{14} photons s^{-1}; this value is insensitive to the position of the emitting dipoles within the device. We thus estimate that $83 \pm 7\%$ of excitons are formed as singlets at 10 K, and, as mentioned earlier, this fraction is independent of drive voltage. Since we have neglected the additional non-radiative processes due to the cathode in the LED structure [23], our value is likely to be an underestimate of the true fraction of singlets. Even taking into account the uncertainties in the triplet–triplet absorption cross-section and in the determination of the singlet generation rate, our results clearly show that the 25% limit is broken, in contrast with results on LEDs based on phosphorescent molecules [24,25]. We note that to break the 25% limit requires not only spin-dependent recombination rates for polaron pairs (which have been predicted and measured [26–28]) but also a mechanism for randomizing the spin states of spin-correlated polaron pairs, for example by dissociation and subsequent recombination with other carriers. This may be more likely in conjugated polymers since electron delocalization allows a significant exchange energy to develop for distant intra-chain polaron pairs which are only weakly coulombically bound [25].

Triplet excitons can decay by either monomolecular recombination, annihilating with other triplets or interacting with charges. Quenching of triplet excitons by charges has been extensively studied in molecular crystals [29], but little information is available about this process in conjugated polymers. The kinetics of the triplet density, n, can be described by the following rate equation

$$\frac{\mathrm{d}n}{\mathrm{d}t} = g - \frac{n}{\tau} - \gamma n^2 - \kappa n_{\mathrm{ch}} n, \tag{2}$$

where g is the triplet generation rate, τ is the monomolecular lifetime, is the triplet–triplet annihilation rate constant γ, and κ is the rate constant for decay by interaction with charges present at a concentration n_{ch}. The frequency dependence of our triplet signal is consistent with monomolecular decay, but with a lifetime which depends on the drive voltage. Fig. 5 shows that there is a linear relationship between decay rate and the charge density determined from the strength of the low-energy polaron feature. Models incorporating significant amounts of triplet–triplet annihilation do not reproduce our data well. The observed behavior therefore provides clear evidence for triplet annihilation by charges being a significant decay mechanism in our devices. By fitting our data to Eq. 2, we determine a rate constant for this interaction of $\kappa = 3 \times 10^{-14}$ cm^3 s^{-1} at 10 K. This rate constant is four orders of magnitude smaller than values reported for anthracene at room temperature [29], due to the lower mobilities of charges and triplet excitons in conjugated polymers than in molecular crystals.

In support of the analysis above, we have ruled out any significant change in monomolecular lifetime due to voltage-dependent heating by using the emission spectrum as a probe of internal temperature of the device [30]. At low temperatures, the decay of charge density at device turn-off is considerably slower than the triplet decay, and we may therefore assume that the charge density is

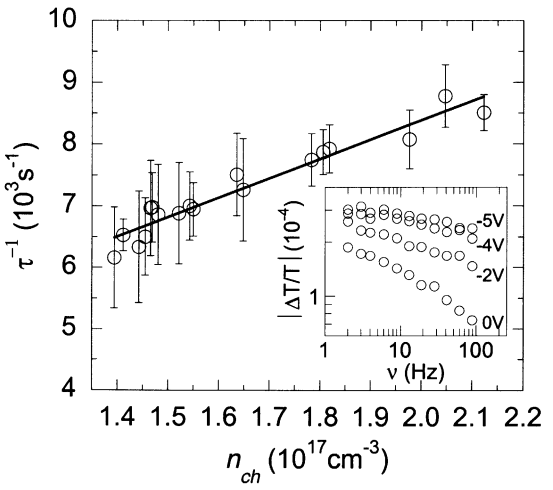

Fig. 5. Triplet decay rate as a function of charge density inside an LED with a 50 nm thick polymer layer. The triplet lifetime was extracted from monomolecular decay fits to the frequency dependent data between 2 Hz and 4 kHz. There was no significant change in the EL over this frequency range. The error bars indicate the uncertainty in the lifetime fitting process. The charge density was calculated from the measured low-energy polaron absorption using the cross-section obtained at room temperature. The inset shows the frequency dependence of the low-energy polaron feature for 6.9 V forward bias and varying negative sweep-out voltages.

constant during the triplet decay. This slow decay, however, complicates the determination of the charge density, since charges may not be completely absent from the device during the off period. The resultant dependence of the polaron signal on modulation frequency can be removed at low frequencies by applying a reverse bias during the off period to sweep out the charges more rapidly (Fig. 5, inset). Charge densities in Fig. 5 were therefore determined using low-frequency data with an reverse bias, such that charges in the device during the off period were not significant.

We have shown that optical spectroscopy of sub-gap absorptions in working polymer LEDs allows quantitative information to be obtained about the formation and decay of excited states. We have identified and separated features due to polarons and triplet excitons, and can quantify their populations, generation rates and decay rates. We provide direct evidence of space-charge-limited currents in polymer LEDs, and hence obtain the absorption cross-section of polaronic charges. We have shown that the population of triplet excitons is significantly smaller than is expected using simple spin-statistics models, and that annihilation by charges is an important decay mechanism for triplet excitons at low temperatures. Our results show that this technique provides a greater depth of information about physical processes in polymer LEDs than can be obtained simply by measuring the current and light output from the devices.

Acknowledgements

This work was partially supported by the NEDO International Joint Research Grant Program, the Engineering and Physical Sciences Research Council, UK, the Belgian Federal Government 'Inter-University Pôle d'Attraction in Supramolecular Chemistry and Catalysis (PAI 4/11)', and by the Belgian National Fund for Scientific Research (FNRS), of which D.B. is a Research Fellow.

References

[1] R.H. Friend, R.W. Gymer, A.B. Holmes, J.H. Burroughes, R.N. Marks, C. Taliani, D.D.C. Bradley, D.A. dos Santos, J.L. Bredas, M. Logdlund, W.R. Salaneck, Nature 397 (1999) 121.
[2] L.S. Swanson, J. Shinar, A.R. Brown, D.D.C. Bradley, R.H. Friend, P.L. Burn, A. Kraft, A.B. Holmes, Phys. Rev. B 46 (1992) 15072.
[3] A.R. Brown, N.C. Greenham, J.H. Burroughes, D.D.C. Bradley, R.H. Friend, P.L. Burn, A. Kraft, A.B. Holmes, Chem. Phys. Lett. 200 (1992) 46.
[4] V. Cleave, G. Yahioglu, P. Le Barny, R.H. Friend, N. Tessler, Adv. Mater. 11 (1999) 285.
[5] Y. Cao, I.D. Parker, G. Yu, C. Zhang, A.J. Heeger, Nature 397 (1999) 414.
[6] P.K.H. Ho, J.S. Kim, J.H. Burroughes, H. Becker, S.F.Y. Li, T.M. Brown, F. Cacialli, R.H. Friend, Nature 404 (2000) 481.
[7] J.S. Kim, P.K.H. Ho, N.C. Greenham, R.H. Friend, J. Appl. Phys. 88 (2000) 1073.
[8] N.C. Greenham, J. Shinar, J. Partee, P.A. Lane, O. Amir, F. Lu, R.H. Friend, Phys. Rev. B 53 (1996) 13528.
[9] M. Redecker, H. Bässler, Appl. Phys. Lett. 69 (1996) 70.

[10] V.G. Kozlov, P.E. Burrows, G. Parthasarathy, S.R. Forrest, Appl. Phys. Lett. 74 (1999) 1057.
[11] N. Tessler, N.T. Harrison, R.H. Friend, Adv. Mater. 10 (1997) 64.
[12] I.H. Campbell, D.L. Smith, C.J. Neef, J.P. Ferraris, Appl. Phys. Lett. 78 (2001) 270.
[13] X. Wei, Z.V. Vardeny, N.S. Sariciftci, A.J. Heeger, Phys. Rev. B 53 (1996) 2187.
[14] D.S. Ginger, N.C. Greenham, Phys. Rev. B 59 (1999) 10622.
[15] M.G. Harrison, K.E. Ziemelis, R.H. Friend, P.L. Burn, A.B. Holmes, Synth. Met. 55 (1993) 218.
[16] L.P. Candeias, G. Padmanaban, S. Ramakrishnan, Chem. Phys. Lett. 349 (2001) 394.
[17] A.P. Monkman, H.D. Burrows, M.D. Miguel, I. Hamblett, S. Navaratnam, Chem. Phys. Lett. 307 (1999) 303.
[18] V. Cleave, G. Yahioglu, P. Le Barny, D.H. Hwang, A.B. Holmes, R.H. Friend, N. Tessler, Adv. Mater. 13 (2001) 44.
[19] Z. Shuai, J.L. Brédas, Phys. Rev. B 62 (2000) 15452.
[20] R.J. Bartlett, J. Phys. Chem. 93 (1989) 1697.
[21] To ensure size consistency, the number of p orbitals included in the active space was raised from 16 for $N=3$ to 34 for $N=7$.
[22] L.P. Candeias, J. Wildeman, G. Hadziioannou, J.M. Warman, J. Phys. Chem. B 104 (2000) 8366.
[23] P.W.M. Blom, M. Vissenberg, J.N. Huiberts, H.C.F. Martens, H.F.M. Schoo, Appl. Phys. Lett. 77 (2000) 2057.
[24] M.A. Baldo, D.F. O'Brien, M.E. Thompson, S.R. Forrest, Phys. Rev. B 60 (1999) 14422.
[25] J.S. Wilson, A.S. Dhoot, A. Seeley, M.S. Khan, A. Köhler, R.H. Friend, Nature 413 (2001) 828.
[26] M. Wohlgenannt, K. Tandon, S. Mazumdar, S. Ramasesha, Z.V. Vardeny, Nature 409 (2001) 494.
[27] Z. Shuai, D. Beljonne, R.J. Silbey, J.L. Brédas, Phys. Rev. Lett. 84 (2000) 131.
[28] M.N. Kobrak, E.R. Bittner, Phys. Rev. B 62 (2000) 11473.
[29] M. Pope, C.E. Swenberg, Electronic Processes in Organic Crystals and Polymers, Oxford University Press, Oxford, 1999.
[30] N. Tessler, N.T. Harrison, D.S. Thomas, R.H. Friend, Appl. Phys. Lett. 73 (1998) 732.